Sedimentology (2001) **48,** 465–478

Hyperpycnal plume formation from riverine outflows with small sediment concentrations

JEFFREY D. PARSONS,*[1] JOHN W. M. BUSH† and JAMES P. M. SYVITSKI‡
*Departments of *Earth, Atmospheric and Planetary Sciences, and*
†Mathematics, MIT, Cambridge, MA 02139, USA
‡INSTAAR, Department of Geological Sciences, University of Colorado, Boulder, CO 80309, USA

ABSTRACT

A series of laboratory experiments has been conducted in order to elucidate the sediment-induced mixing processes accompanying riverine outflows; specifically, the discharge of a warm, fresh, particle-laden fluid over a relatively dense, cool brine. In a parameter regime analogous to recently acquired field measurements, hypopycnal (surface) plumes were subject to a convective instability driven by some combination of heat diffusing out of the warm, fresh, sediment-laden plume and particle settling within it. Convection was robust in the presence or absence of intense turbulence, at sediment concentrations as low as 1 kg m^{-3}, and took the form of millimetre-scale, sediment-laden fingers descending from the base of the surface plume. A consequence of the convective instability of the original hypopycnal plume is the generation of a hyperpycnal (bottom-riding) flow. The experiments presented here indicate that natural river outflows may thus generate hyperpycnal plumes when sediment concentrations are 40 times less than those required to render the outflow heavy relative to the oceanic ambient. The resulting hyperpycnal plumes may play an important role in transporting substantial quantities of sediment to the continental slope and beyond.

Keywords convective sedimentation, cross-shelf transport, fingers, plumes.

INTRODUCTION

When a river enters the ocean, it can generate a hypopycnal plume, which remains at the surface, or a hyperpycnal plume, which descends to the sea floor as a result of the excess density generated by its sediment load. Hyperpycnal plumes are a class of sediment-laden gravity current, commonly referred to as turbidity currents. The resulting turbidite deposits are found in many marine sediments around the world (e.g. Normark *et al.*, 1993; Kneller, 1995), and hyperpycnal plumes provide a simple explanation for their prevalence.

A commonly accepted criterion for hyperpycnal plume generation from riverine outflows is that the bulk density of a river exceeds that of the oceanic ambient (Mulder & Syvitski, 1995). As river outflows are typically fresh and warm relative to the ocean, such a criterion requires sediment concentrations approaching 40 kg m^{-3}. According to this criterion, only a few small rivers in mountainous terrain are capable of producing hyperpycnal plumes annually (Mulder & Syvitski, 1995). However, even large rivers on passive margins (e.g. the Amazon) have developed large turbidite fans during the Quaternary (Imran *et al.*, 1999).

Perhaps the most widely accepted explanation of turbidite formation relies on the conversion of submarine failures caused by earthquakes (Beattie & Dade, 1996) or 'oversteepening' (Syvitski & Hein, 1991; Zeng *et al.*, 1991) to turbidity currents.

[1] Present address: University of Washington, School of Oceanography, Seattle, WA 98195-7940, USA (E-mail: parsons@ocean.washington.edu)

However, Maar (1999) has shown that the conversion of failure-generated debris flows and landslides to dilute turbidity currents is an inefficient process (i.e. large debris flows are required to produce relatively small turbidites). Resolving the importance of hyperpycnal plumes in the formation of turbidite fans is therefore a fundamental problem in submarine geomorphology. Source location and continuity of sediment supply are important factors in determining the location and prevalence of turbidite fans, as well as their surface morphology and internal architecture.

When sediment is considered as a contributor to the density of a continuous fluid phase (as are temperature and salinity), then it becomes evident that gradients in sediment concentration may prompt convection. The sediment fluxes associated with convective transport may dominate those associated with discrete particle settling (Bradley, 1965). Such could be the case in the settling of fine sediment from riverine outflows, where the time-scale of individual particle settling is of the order of a week to a year, depending on flocculation rates. Flocculation, a complex aggregation phenomenon that can produce relatively large sediment settling rates under certain conditions, has been studied extensively (Syvitski & Murray, 1981; Hill & Nowell, 1995; Hill *et al.*, 1998). Although flocculation may play an integral role in sediment-laden plume dynamics, it is not necessarily the most efficient mechanism by which sediment can leave surface waters.

In recent years, there has been a growing awareness of the capability of other sedimentation processes to affect river plume dynamics. Various researchers have examined the importance of double-diffusive sedimentation (DDS), which arises in the gravitationally stable situation where warm, sediment-laden fluid overlies a denser, cooler ambient (Green, 1987; Chen, 1997; Hoyal *et al.*, 1999a; Parsons & García, 2000). The classic form of double-diffusive convection (DDC) is salt-fingering, a well-studied and well-documented mode of thermohaletal convection that is prevalent in the oceans when warm salty water overlies a relatively dense, cold ambient (Schmitt, 1994). Salt-fingering relies on the large difference in the diffusivities of heat (10^{-7} m^2 s^{-1}) and salt (10^{-9} m^2 s^{-1}) and is characterized by millimetre-scale laminar plumes, termed salt fingers. DDS may be understood as a direct analogue of salt-fingering, with sediment now playing the role of the slower diffusing component, and is similarly characterized by millimetre-scale, finger-like plumes.

'Settling convection' results from gradients in particle concentration that give rise to gravitationally unstable configurations (Keunen, 1968; Hoyal *et al.*, 1999b). Hoyal *et al.* (1999b) performed experiments that investigated the convection associated with a mechanically mixed, fresh, sediment-laden layer (concentrations varying between 0·3 and 15 kg m^{-3}) overlying a relatively dense, sugar-laden ambient. The sediment settles into the lower layer, giving rise to a gravitationally unstable situation in the lower layer: a sediment-laden boundary layer grows at the top of the lower layer until the release of negatively buoyant plumes. The photographs from Hoyal *et al.* (1999b) illustrate a horizontal sediment-laden interface punctuated by sinking plumes, which appear as thin (millimetre-scale) cusps separated by at least 1 cm. This form of convection is quite distinct from DDS, in which the plumes are space-filling and finger-like.

Maxworthy (1999) investigated surface gravity currents with high sediment concentrations (>15 kg m^{-3}) supported by a strong salinity gradient (>1·7% of the total density) and observed convection in the form of vigorous centimetre-scale turbulent plumes. Maxworthy (1999) noted that, for sediment concentrations below ≈10–15 kg m^{-3} [greater than any of the experiments of Hoyal *et al.* (1999b)], convection was not significant, an observation consistent with other saline-supported gravity current experiments (Parsons, 1998). Maxworthy (1999) interpreted the observed instability as resulting from the development of a relatively thin (centimetre-thick) boundary layer of concentrated sediment and mixed ambient fluid at the base of the current. The boundary layer ultimately becomes gravitationally unstable and initiates convection, and its thickness is related to the scale of the descending sediment-laden plumes.

Each of the aforementioned studies has made clear the potential importance of particle-driven convective transport from riverine outflows. However, an experimental investigation has yet to be performed in the parameter regime most relevant to oceanic riverine outflows: conditions in which temperature, salinity and sediment concentration all impact the dynamics of the surface layer. This article presents the results of the first such experimental investigation, which demonstrates that sediment-driven convection is capable of generating hyperpycnal plumes in realistic natural scenarios with significantly less sediment than is required by traditional models (Mulder & Syvitski, 1995). The ramifications of

sediment-driven convection are also discussed with respect to the characteristics observed at the mouths of the world's rivers.

EXPERIMENTAL SET-UP AND PROCEDURE

Two series of laboratory experiments were performed in order to elucidate the physical processes responsible for sedimentation from an initial hypopycnal plume. In the Ven T. Chow Hydrosystems Laboratory at the University of Illinois at Urbana-Champaign, experiments were performed in order to investigate sedimentation from a warm, fresh, surface gravity current. This series of experiments will hereafter be referred to as Series 1. A diagram of the experimental apparatus is shown in Fig. 1.

Series 1 experiments were performed by discharging 400 mL of warm, fresh, sediment-laden source fluid over a cool, salty ambient. After the source fluid was well mixed and poured into the source box, the gate on the source box was released. Lock-exchange, fixed-volume gravity currents are characterized by a constant Froude number $Fr_c = U_c/\sqrt{\delta g h_c}$ of order 1 (Huppert & Simpson, 1980), where U_c is the velocity of the current front, g is the acceleration resulting from gravity, h_c is the height of the current, and δ is the dimensionless density difference between the gravity current and the ambient, henceforth

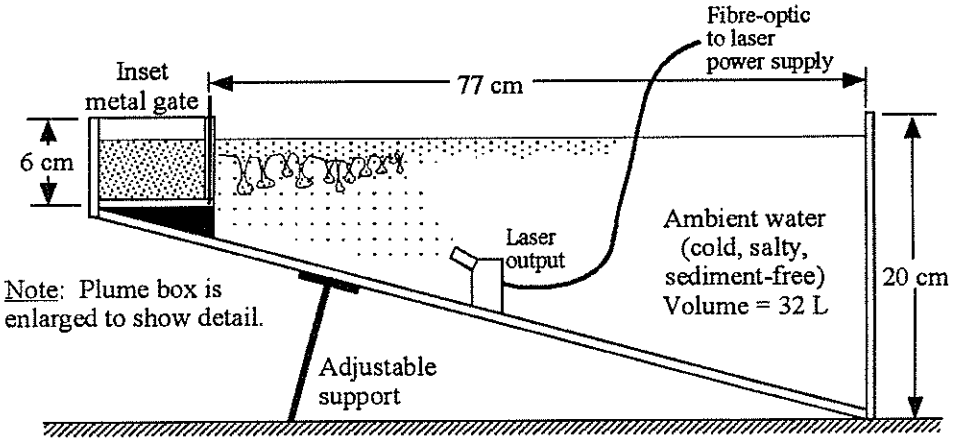

Fig. 1. Laboratory apparatus for the Series 1 experiments.

referred to as the overall stratification. Specifically, $\delta = \alpha\Delta T + \beta\Delta S - \beta' C$, where ΔT and ΔS are the temperature and salinity differences, C is the volumetric sediment concentration, α and β convert temperature differences to excess density differences, and β' is the submerged specific gravity of the sediment. The current Reynolds numbers, $Re_c = U_c h_c / \nu$, where ν is the kinematic viscosity, were typically of the order of 1000. At these Reynolds numbers, gravity current mixing processes are not fully turbulent; however, there is still substantial mixing between the two fluid masses.

A second series of experiments was performed in the Fluid Dynamics Laboratory of the Mathematics Department at MIT in order to examine the evolution of an initially quiescent two-layer system. The experimental conditions (a warm, fresh, sediment-laden layer overlying a cool brine) were qualitatively similar to those examined in the Series 1 experiments; however, the interface between the two layers lacked shear. The method used was originally implemented by Dalziel (1993) to produce optimal initial conditions for an experimental investigation of the Rayleigh–Taylor problem (i.e. the collapse of a gravitationally unstable, two-layer system). A diagram of the device is shown in Fig. 2.

The experiment is initiated by pulling two pieces of cloth out of the tank, which in turn withdraws two thin (1 mm) welded aluminium plates, thus removing the dividing wall while minimizing relative motion between the wall and the ambient fluid. The Series 2 experiments allowed the examination of sediment-induced convective instability in the absence of shear between the two layers and permitted accurate control and measurement of the properties (e.g. temperature, salinity and sediment concentration) of the two fluid phases. It is noteworthy that several experiments were performed without the cloth gate mechanism (i.e. simply by withdrawing a thin, single horizontal plate), and no substantial difference in behaviour was observed. Typically, the time-scale of disturbances associated with withdrawal of the plate was short relative to that for the initiation of sediment-driven convection.

The particles used were highly angular silica grains processed by US Silica (Ottawa, IL, USA). Several different products were used. In all the Series 1 and some Series 2 experiments, sediment with a mean grain size of 6·5 μm (SIL-CO-SIL 40) was used. The mean settling speed of these particles is 0·03 mm s^{-1}, which corresponds to particle Reynolds numbers ($Re_p = v_s D_{50}/\nu$, where v_s is the Stokes settling speed and D is the mean particle size) less than 10^{-3}. Other experiments used SIL-CO-SIL 250 and SIL-CO-SIL 106, which have mean grain sizes of ≈ 45 and 17 μm respectively. A few Series 2 experiments were performed using ballotini (manufactured blown silica) with a mean grain size of 30 μm.

EXPERIMENTAL RESULTS

In the Series 1 experiments, the spreading surface current was the source of sediment-driven convection in all runs. Flow parameters were chosen

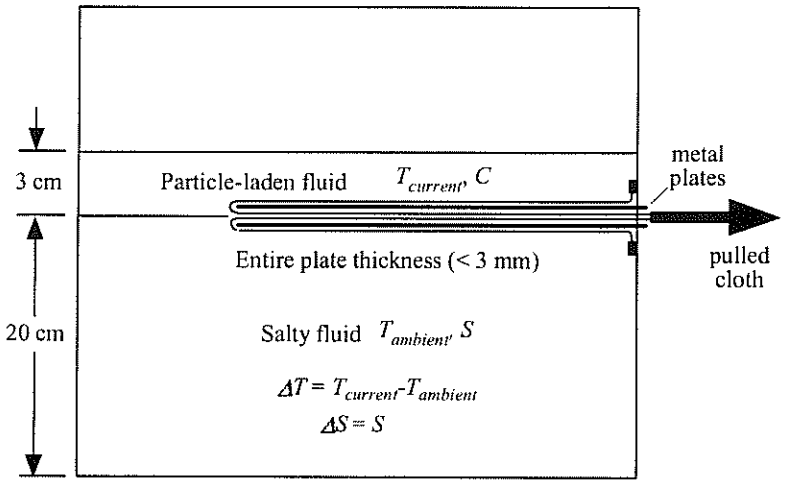

Fig. 2. Laboratory apparatus for the Series 2 experiments.

to correspond to conditions in the Eel River plume (Morehead & Syvitski, 1999). The sediment-laden surface layers were supported by a strong, positive salinity gradient ($\beta\Delta S > 0{\cdot}01$) and an appreciable stabilizing temperature difference ($\Delta T = 5$–20 °C). The source box conditions are reported in Table 1; however, it is noteworthy that the resulting surface layer in the Series 1 experiments may be diluted substantially by mixing across the gravity current interface.

In all the Series 1 experiments, propagation of the initial, surface-riding gravity current was slowed by finger-like convection. The early stages of these experiments were similar to those reported by Maxworthy (1999), in which a sediment laden gravity current over-running a fresh ambient produced large convective plumes [Fig. 3a (ii) and (iii)]. Subsequently, convection persisted in the form typified by millimetre-scale, particle-laden, finger-like plumes emerging from the base of the upper layer [Fig. 3a (iv)]. This latter form of convective behaviour will hereafter be referred to as 'finger convection', in order to distinguish it from settling convection and classic, two-component, double-diffusive sedimentation.

Only in the experiments showing the weakest convection (expts 4, 6 and 7; Table 1) did the head of the initial gravity current reach the far end of the tank. Typically, the momentum of the current was lost to the convecting fingers, and a small, stagnant, sediment-laden surface layer remained in the vicinity of the source box. Previous investigations of double-diffusive gravity currents (Maxworthy, 1983) and rapidly sedimenting particle-laden gravity currents (Maxworthy, 1999) have reported similar behaviour. As in these previous studies, the sediment-driven convection in the Series 1 experiments typically spawned a bottom turbidity current, or hyperpycnal plume [Fig. 3a (iv)]. These currents were extremely dilute, but moved at moderate speeds (1–10 cm s^{-1}) over the bottom slope of the box. The final state of most experiments (expts 4, 6 and 7 are exceptions) was a turbidity current with a small remnant surface layer feeding it by finger convection. Figure 3b qualitatively illustrates the process of turbidity current formation by this mechanism.

The fall velocity of the fingers was recorded from digitized video camera images and related to the sediment concentration in the source box (Table 1, Fig. 4). Suspensions with concentrations in excess of 10–15 kg m^{-3} were difficult to maintain without significant settling in the source box, whereas more dilute flows developed too slowly to produce significant convection. Within this limited parameter range, measured finger speeds were comparable with, or exceeded, settling speeds produced by large, well-developed flocs (>100 μm; Sternberg *et al.*, 1999). This observation underlines the potential importance of finger convection in sedimentation from riverine outflows. The observed finger speeds should not be linearly related to the source sediment concentration (as would be expected in the case of classic, two-component DDS) owing to the influence of the salinity jump at the interface in altering the constitutive properties of the fingers (i.e. both their sediment concentration and their salinity).

The Series 2 experiments revealed the prevalence of convection over an extremely wide range of conditions in the absence of ambient turbulence (Table 2). Unlike the Series 1 experiments,

Table 1. Results from the gravity current interface (Series 1) experiments.

Experiment	$\alpha\Delta T$	$\beta\Delta S$	U (cm s^{-1})	$\beta'C$	R	R_s
1	0·0042	0·01	0·33	0·00512	2·8	2·0
2	0·0026	0·01	0·22	0·00446	2·8	2·2
3	0·0041	0·01	0·40	0·00778	1·8	1·3
4	0·0069	0·01	0·091	0·00351	4·8	2·8
5	0·0059	0·005	0·42	0·00621	1·8	0·8
6	0·0059	0·02	0·034	0·00244	10·6	8·2
7	0·0064	0·01	0·018	0·00169	9·7	5·9
8	0·0022	0·02	0·36	0·00734	3·0	2·7
9	0·0056	0·02	0·32	0·00502	5·1	4·0
10	0·0032	0·005	0·24	0·00596	1·4	0·8

$\alpha\Delta T$, $\beta\Delta S$ and $\beta'C$ are the temperature, salinity and sediment contributions to the density respectively. U is the mean velocity of the convective fingers. $R = (\alpha\Delta T + \beta\Delta S)/\beta'C$ is the density-difference ratio. $R_s = \beta\Delta S/\beta'C$ is a measure of the stability of the plume with the stabilizing temperature gradient removed.

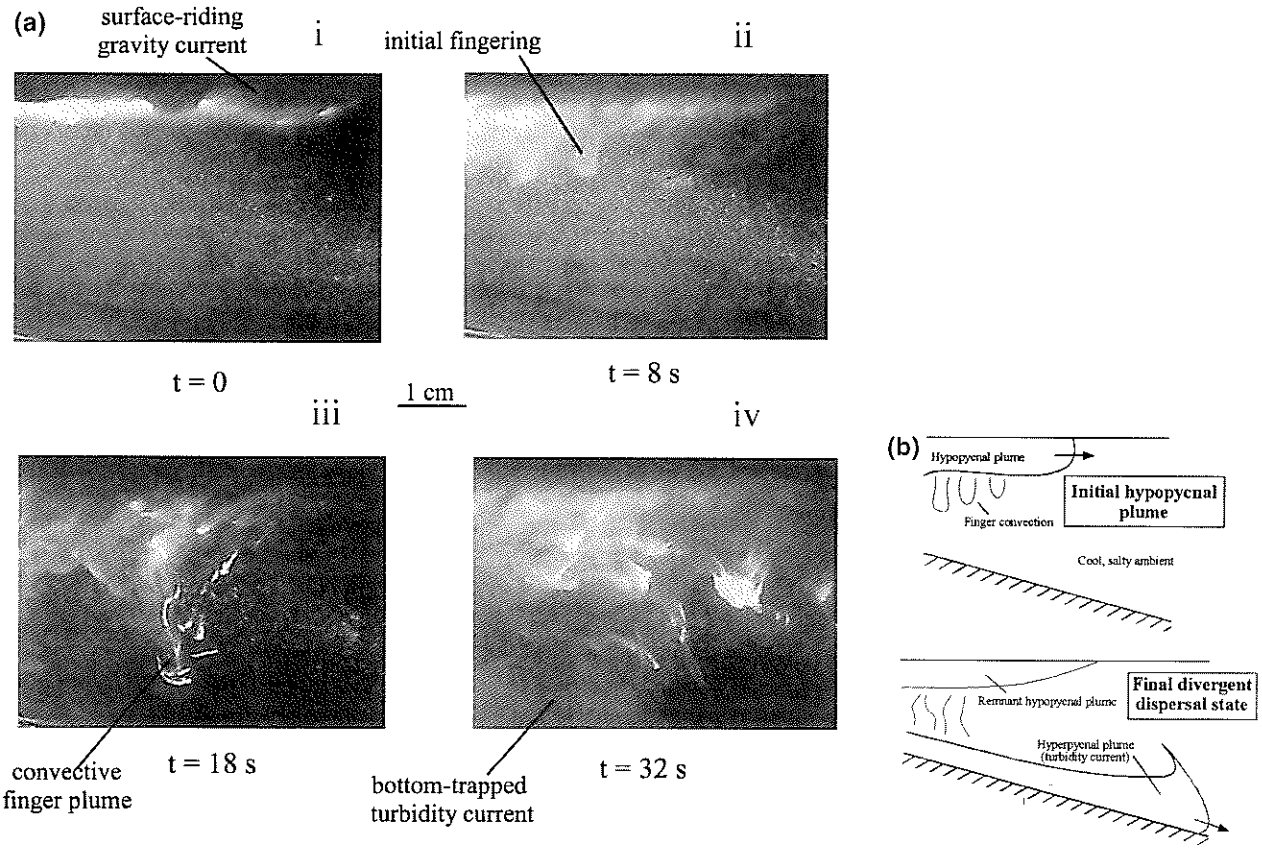

Fig. 3. (a) Sequence of photographs from a strongly scavenged plume. The sequence was obtained from Series 1, expt 8. Although it is difficult to observe, a turbidity current moves from left to right with a velocity in excess of 1 cm s^{-1}. (b) A schematic diagram of the hyperpycnal plume formation process observed in the experiments.

two distinct modes of convective instability were observed. As is evident in Figs 5 and 6, the two modes of convection, 'leaking' and 'fingering', were easily distinguished by their appearance.

The first form of convective behaviour observed in the Series 2 experiments was identical to the finger convection observed in the later stages of the Series 1 experiments and arose in a large parameter range, within which both temperature and salinity were stabilizing. As illustrated in Fig. 5, the finger convection is strongly reminiscent of DDS, being similarly characterized by space-filling, millimetre-scale laminar finger plumes.

The second mode of convection observed, referred to as 'leaking', was similar in appearance to the 'settling-driven convection' reported by Hoyal *et al.* (1999b) and markedly different from the finger convection observed in the Series 1 experiments. Figure 6a demonstrates that leaking is characterized by millimetre-scale, sinking sheet plumes. When illuminated by a vertical light sheet, the flow is characterized by a number of discrete millimetre-scale laminar plumes descending from the interface, giving the interface a cusp-like appearance. The cusps are separated by a few centimetres and typically translate along the interface. When observed in plan view with a horizontal light sheet, the sheets assume the form of an irregular polygonal pattern (Fig. 6B and C). The absence of leaking in the gravity-current (Series 1) experiments suggests that it is not robust in the presence of interfacial turbulence.

Figure 7 summarizes the results of the Series 2 experiments. Systems marked by sufficiently low sediment concentrations (C_{mass} <1 kg m^{-3}) and large density difference ratios [$R = (\alpha\Delta T + \beta\Delta S)/\beta' C < 100$] did not initiate convective instability; that is, the sediment settled as individual grains through the lower layer at the Stokes settling speed. Consequently, the sediment-laden layer expanded at approximately the rate prescribed by the Stokes settling speed of the sediment (0·03 mm s^{-1} in the case of the 6·5-μm particles). This expansion persisted for as long as any experiment was observed (up to 1 h) without prompting convective overturning. When the upper layer was cool relative to the lower layer,

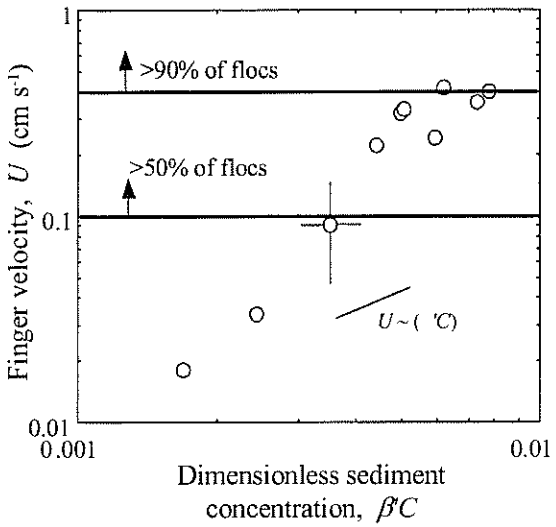

Fig. 4. Convective finger velocity vs. dimensionless sediment concentration. Flocculated settling rates are obtained from Sternberg *et al.* (1999). Lines correspond to the 50th and 90th percentile of settling speeds. Error bars on expt 5 are characteristic of all runs (50% for the finger velocity, 20% for the sediment concentration in the source box). Error estimates of the finger velocity represent the standard deviation of the individual finger speeds measured. At least 10 fingers were examined for each experimental run, and the data (circles) represent the averaged values.

only leaking convection was observed. At higher concentrations and when the upper layer was warm, the principal mode of convection changed from leaking to fingering (Fig. 7). An unexpected feature of the experiments was that, in the limit of large stabilizing temperature differences, convection returned to a leaking planform.

Nearly all the Series 1 experiments were performed in the parameter range at which 'fingering' was observed in the Series 2 experiments; however, caution should be applied in relating the parameters directly. The parameters describing the source fluid in the Series 1 experiments may not accurately describe the surface layer (ΔS, ΔT, C) owing to the influence of gravity current mixing processes. Dilution by these mixing processes is most probably responsible for the lone outlier: Series 1, expt 7. For the sake of comparison, however, the Series 1 experiments are plotted alongside the Series 2 experiments in Fig. 7.

ANALYSIS AND DISCUSSION

Previous work has shown that significant sediment transport could be induced by double-

Table 2. Experimental conditions for the Series 2 experiments.

Expt	$T_{ambient}$	$T_{current}$	$\beta\Delta S$	C_{mass}	D_{50}	Form of motion
1	20·5	41	2	3	6·5	Fingers
2	20	42	2	3	45	Fingers
3	22	42	2	4	45	Fingers
4	21	40	2	4	6·5	Fingers
5	20·5	45	2	3	45	Fingers
6	21	45	2	3	6·5	Fingers
7	21	21	2	3	45	Intermediate
8	21	21	2	3	6·5	Leaking
9	21	21	1·5	5	6·5	Leaking
10	21·5	31	1	4	45	Fingers
11	22	30	1·4	5	45	Leaking
12	22	27	0·7	3·5	6·5	Intermediate
13	21·5	14·5	2	3	45	Leaking
14	17	22	2	3	45	Intermediate
15	23	29	1·2	5	6·5	Intermediate
16	22	22	1·1	4	45	Intermediate
17	22	15	2	3	6·5	Leaking
18	22	33	1	4	6·5	Fingers
19	23	49	0	0·6	6·5	Fingers
20	23	31	0	0·6	6·5	Fingers
21	23	5	2	3	6·5	Leaking
22	23	36	2	3	6·5	Fingers
23	23	27	2	3	6·5	Intermediate
24	23	33	2	2	6·5	Fingers
25	20	24	2	2	6·5	Intermediate
26	23	24	2	2	6·5	Leaking
27	23	16	2	2	6·5	Leaking
28	23	44	2	5	6·5	Fingers
29	23	27	2	4	6·5	Fingers
30	23	4	2	5	6·5	Leaking
31	23	23	2	4	6·5	Intermediate
32	23	21	2	4	6·5	Leaking
33	23	23	2	5	6·5	Intermediate
34	24	36	2	5	6·5	Fingers
35	24	24	2	1	6·5	Leaking
36	24	29	2	1	6·5	Fingers
37	24	26	2	1	6·5	Intermediate
38	23	31	2	5	6·5	Intermediate
39	23	50	2	6	6·5	Fingers
40	25	4	2	6	6·5	Leaking
41	24	29	2	6	6·5	Intermediate
42	24	37	2	6	6·5	Fingers
43	24	24	2	6	6·5	Intermediate
44	24	19	2	6	6·5	Leaking
45	24	35	2	6	6·5	Fingers
46	24	44	2	2	6·5	Leaking
47	24	24	2	0·5	6·5	Leaking
48	20	25	2	2	6·5	Fingers
49	24	34	2	2	6·5	Leaking
50	24	44	2	0·5	6·5	No convection
51	24	44	2	1	6·5	No convection
52	24	4	2	1	6·5	Leaking
53	24	4	2	0·5	6·5	Leaking
54	24	55	2	5	6·5	Intermediate
55	24	66	2	6	6·5	Leaking
56	24	36	2	1	6·5	Leaking

Table 2. Continued.

Expt	$T_{ambient}$	$T_{current}$	$\beta\Delta S$	C_{mass}	D_{50}	Form of motion
57	24	33	2	1	6·5	Leaking
58	24	31	2	0·5	6·5	Leaking
59	24	36	2	0·5	6·5	Leaking
60	24	38	2	0·5	6·5	No convection
61	24	29	2	0·5	6·5	Leaking
62	21	36	2	1	6·5	No convection
63	21	54	2	2	6·5	Leaking
64	21	33	1·3	2·5	6·5	Fingers
65	21	28	1·4	2·5	6·5	Intermediate
66	21	38	1·5	2·5	6·5	Intermediate
67	22	35	1	2·5	6·5	Intermediate
68	22	40	1	2·5	6·5	Intermediate
69	22	40	1·2	2·5	6·5	Leaking
70	22	32	2	2·5	6·5	Intermediate
71	22	65	2	3	6·5	Leaking
72	22	58	2	4	6·5	Intermediate
73	22	52	2	3	6·5	Leaking
74	22	52	2	4	6·5	Intermediate
75	22	44	2	2·5	6·5	Leaking
76	22	40	2	2·5	6·5	Intermediate
77	22	37	2	2·5	6·5	Fingers
78	22	34	2	2·5	6·5	Fingers
79	22	29	2	2·5	6·5	Intermediate
80	22	22	2	2·5	6·5	Leaking
81	22	65	2	2·5	6·5	Leaking
82	22	22	0·4	2·5	6·5	Fingers
83	21	7	2	2·5	6·5	Leaking
84	21	7	1·4	2·5	6·5	Leaking
85	21	14	0·4	2·5	6·5	Leaking
86	21	13	1	2·5	6·5	Leaking
87	21	12	2·9	2·5	6·5	Leaking
88	21	39	0·4	2·5	6·5	Intermediate
89	21	39	2·5	2·5	6·5	Fingers
90	21	37	0·2	2·5	6·5	Fingers
91	21	45	0·2	2·5	6·5	Fingers
92	20	20	1·6	2·5	6·5	Intermediate
93	20	20	1·1	2·5	6·5	Leaking
94	20	45	0	2·5	6·5	Fingers
95	21	64	2	3	45	Leaking
96	20	49	2	3	45	Intermediate
97	15	15	2	3	19	Leaking
98	15	5	2	3	19	Leaking
99	15	65	2	3	19	No convection
100	19	30	2	3	19	Intermediate
101	15	28	2	3	45	Fingers
102	13	32	2	3	19	Intermediate
103	12	44	2	3	19	Fingers
104	19	60	2	3	19	Leaking
105	16	51	2	3	19	Intermediate
106	15	54	2	3	19	Leaking
107	13	40	2	3	19	Fingers
108	13	36	2	3	45	Intermediate
109	19	6	2	3	30	Leaking
110	15	15	2	3	30	Leaking
111	13	70	2	3	30	No convection
112	15	26	2	3	30	Intermediate
113	16	47	2	3	30	Intermediate
114	15	35	2	3	30	Fingers
115	16	41	2	3	30	Intermediate
116	16	58	2	3	30	Leaking
117	18	70	2	1	6·5	No convection
118	20	7	2	4	6·5	Leaking
119	21	44	2	4	6·5	Fingers

Variables are defined in Fig. 2. Temperatures are in °C and sediment concentrations in kg m^{-3}. $\beta\Delta S$ is expressed as a percentage. D_{50} is the mean grain size of the sediment used (in microns). All the material is angular silica, with the exception of the ballotini (30 μm), which are spherical. The form of convection is a qualitative measure based upon the characteristics of Figs 5 (leaking) and 6 (fingers).

diffusive convection in a sedimenting system (Green, 1987; Chen, 1997; Hoyal *et al.*, 1999a; Parsons & García, 2000); however, these processes were observed in relatively simple, two-component (temperature and sediment) systems. Hoyal *et al.* (1999a) presented calculations suggesting that isothermal saline-sediment systems cannot produce significant double-diffusive fluxes, a conclusion corroborated by laboratory experiments (Parsons, 1998). Finger convection, on the other hand, is robust across interfaces stabilized by both temperature and salinity, in situations in which the interface is either quiescent (Series 2 experiments) or mixed by shear-induced turbulence (Series 1 experiments). In both cases, it appears that the downward transport of heat and sediment from the upper layer is sufficient to induce convective instability. Figure 8 casts both finger and leaking convection in terms of previous work on convective sedimentation.

Figure 1 of Hoyal *et al.* (1999b) illustrates what would be considered 'leaking'. Although the upper sediment-laden layer was mechanically mixed in the experiments of Hoyal *et al.* (1999b), the stirring did not give rise to mixing across the interface and so was not as vigorous as that expected to arise in a surface gravity current. Despite the relative fragility of leaking convection, it may be extremely important in certain oceanic settings (i.e. nepheloid transport) and will be the subject of further study.

An important aspect of finger convection is that it appears to be robust in the presence of turbulent mixing (as illustrated in the Series 1 experiments). The stability of a stably stratified shear flow is determined by the Richardson

Fig. 5. Photograph of finger convection in a saline-supported layer (Series 2, expt 118); scale increments in mm. Note finger size and the degree of magnification of the image compared with Figs 3a and 6. The photo was taken less than 1 minute after the partition was removed. Finger convection quickly obscured the lower layer and made planform photography futile with the available equipment.

number, $Ri = \delta gh/\Delta U^2$, where ΔU is the velocity difference over a vertical distance h. For Richardson numbers less than 0·25, it has been shown (theoretically: Howard, 1961; experimentally: Thorpe, 1973) that Kelvin–Helmholtz (KH) instability will result and intensify mixing. Most river outflows maintain local Richardson numbers between 0·3 and 0·7, slightly exceeding this critical value (Geyer & Smith, 1987). At the interface of gravity currents, Richardson numbers have been shown to be in this range (between 0·3 and 0·5; Britter & Simpson, 1978; Parsons, 1998). In the Series 1 experiments, finger convection arose in every gravity current studied. On a number of occasions (e.g. Series 1, expts 3, 5 and 8), finger convection would precede and suppress KH development at the front of a gravity current, where Richardson numbers are well below 0·25 (Parsons, 1998). Although additional turbulent processes (e.g. wave-induced mixing) may be significant in the field and cannot be simply modelled in the laboratory, the Series 1 experiments strongly suggest that finger convection will be robust in well-mixed environments.

Flocculation is an important sediment transport process in natural riverine plumes (Syvitski & Murray, 1981; Hill & Nowell, 1995; Hill *et al.*, 1998); however, it was not observed in any of the experiments. At no time were individual grains observed: the sediment-laden fluid always appeared as a cloudy continuum. This observation is in sharp contrast to recent field studies (Sternberg *et al.*, 1999), in which flocs were clearly observed with similar photographic equipment. The absence of flocs in the experiments is consistent with the time-scales associated with the convection observed. Whitehouse *et al.* (1960) reported that it required 20 min to flocculate montmorillonite, a relatively inactive clay, to the point at which the settling velocity was noticeably different from Stokes settling of individual grains. Even the finest sediment used in the experiments should flocculate more slowly (as it is not a clay, but an electrostatically inactive silt), and then only in gently stirred conditions. The coarsest material

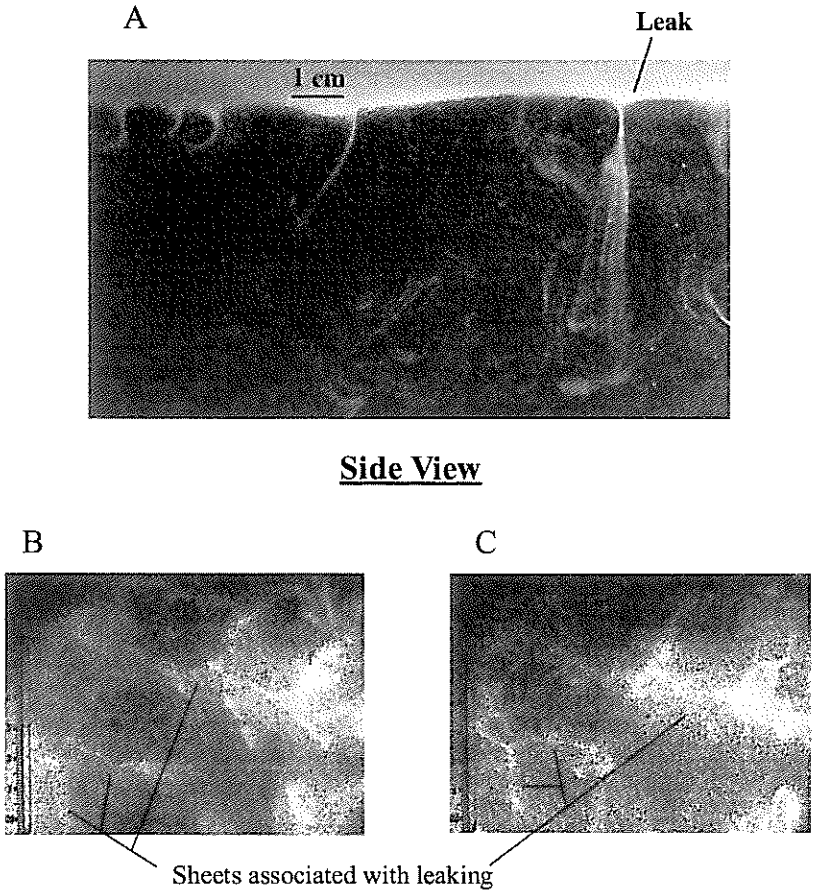

Fig. 6. Photographs of leaking convection taken from Series 2, expt 119. Photo (A) illustrates flow with a vertical (cross-sectional) light sheet, whereas photos (B) and (C) show the planform of the behaviour visualized with a horizontal light sheet. A mirror tilted at 45° was used to observe the planform geometry of the leaking convection. The planform images (B and C) are of poorer quality because light is scattered readily from suspended sediment. The planform photos were taken 5 s apart and together illustrate the observed sheets. Photo (A) was taken approximately 5 min after the initiation of the experiment.

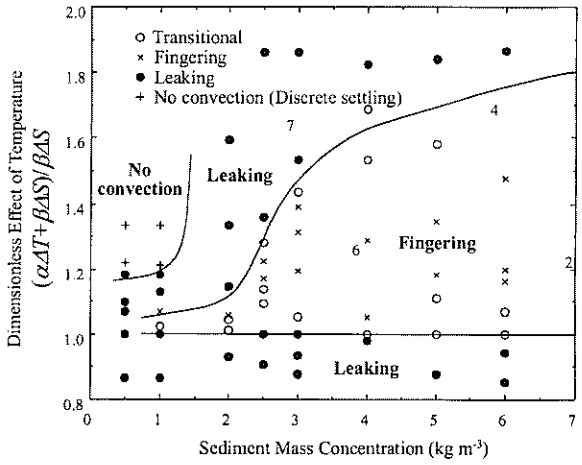

Fig. 7. Regime diagram of the Series 2 experiments. The mass sediment concentration is plotted against the dimensionless effect of temperature for a fixed salinity difference ($\beta\Delta S = 0{\cdot}02$). All experiments shown are salinity dominated ($\beta\Delta S > \alpha\Delta T$, $\beta' C$). Transitional behaviour indicates experiments in which both leaking and fingering modes were observed. Numbers indicate Series 1 experiments. Series 1 experiments not pictured had source sediment concentrations in excess of 7 kg m^{-3}.

used (30-μm ballotini and 45-μm ground silica) should not flocculate under any circumstances owing to its relatively large size and smooth shape.

FIELD IMPLICATIONS

Convection, rather than discrete particle settling, is the dominant mechanism of fine sediment (silt) transport at the laboratory scale in situations analogous to natural river plume conditions. However, extension of this observation to the field is not trivial. Flocculation, for instance, will affect the dynamics of convective processes; however, the converse is also true. The interplay between slowly developing flocculation and relatively rapid convective processes remains an important subject for further study.

Despite the potentially important role of flocculation and discrete settling, field evidence indicates that continuum behaviour is a common feature of fine sediment dynamics on continental shelves. The presence of fluid muds, i.e. concen-

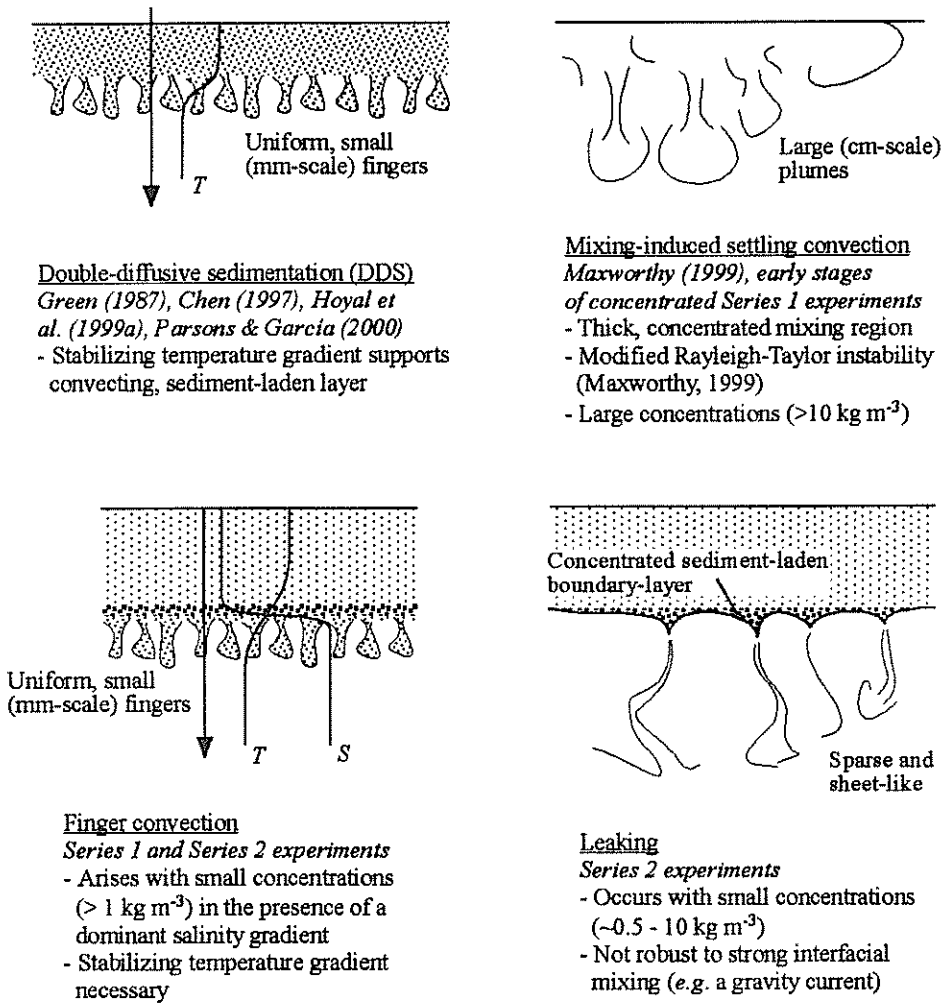

Fig. 8. Schematic summary of the observed behaviour discussed in context with previous work. Vertical temperature (T) and salinity (S) profiles are indicated, along with characteristic flow structures.

trated (>10 kg m^{-3}) fine sediment slurries that display continua properties, has been documented throughout the world (Amazon, Kineke *et al.*, 1996; Papua New Guinea, Kineke *et al.*, 2000; northern California, Ogston *et al.*, 2000). Traditionally, fluid muds have been characterized as flows generated from current and wave-bottom boundary layer shear entraining fine particles from an unconsolidated bed. However, the study presented here suggests that they may also be formed from sediment-driven convection from a surface plume.

It is important to note that the hyperpycnal plumes resulting from finger convection differ dramatically from the traditional conception of these plumes. They must form from an unstable hypopycnal plume, the remnant of which will remain at the surface and may propagate a significant distance seaward. Despite the persistence of the hypopycnal plume, more than half the sediment could be lost to a dense, bottom-riding gravity current. Moreover, it is conceivable that these turbidity currents could initiate larger and faster flows capable of transporting coarser material by the resuspension of particles from the bed (Parker *et al.*, 1986). If the shelf slope and sediment concentration are inadequate for the development of a turbidity current, a fluid mud may result. In either case, the bottom layer would control the sediment dynamics of the estuary–shelf system. The concept of a 'divergent dispersal system' (i.e. a hypopycnal plume coupled to a hyperpycnal flow, as in Fig. 3b) is neither new nor without field observation. Kineke *et al.* (2000) reported a divergent dispersal system at the mouth of the Sepik River, but did not discuss its physical origin at length.

Criterion	Dirty	Moderately dirty	Moderately clean	Clean	Not possible
Mulder & Syvitski (1995)					
C_{mass} = 40 kg m^{-3}	9	72	24	13	29
C_{mass} = 5 kg m^{-3}	61	48	15	8	15

Table 3. The change in the characterization of rivers when the influence of convective sedimentation is considered.

The 147 rivers discussed in Mulder & Syvitski (1995) were reanalysed using a criterion for hyperpycnal plume generation corresponding to that for sediment-driven convection. River categorization is based on Mulder & Syvitski (1995) and is discussed in the text.

Another possible mechanism for seaward transport from a sediment-laden hypopycnal plume was observed in the experiments; specifically, mid-depth nepheloid layers, or interflows. After substantial dilution by convective mixing processes, sediment concentration may contribute relatively little to the fluid density (<10% of the contributions of salinity and temperature), so that mid-depth nepheloid layers may be supported by weak ambient haloclines. Owing to their relative quiescence, halocline-supported nepheloid layers may become unstable to leaking, the initiation and vigour of which will be highly dependent on both sediment concentration and the strength of the supporting halocline (Fig. 5; Hoyal *et al.*, 1999b).

Because direct field confirmation is difficult, analysis has been made to identify the ramifications of convective sediment transport on the dynamics of the world's rivers. To this end, the analysis of Mulder & Syvitski (1995) provides a standard for comparison and extrapolation. Mulder & Syvitski (1995) published tables for 147 rivers, listing the load-averaged mean concentration of suspended sediment $\bar{C} = Q_s/Q$, which was calculated from a global database of mean annual river discharge Q and sediment discharge Q_s. Because sediment transport is a highly non-linear process (García & Parker, 1993), flood values of $\bar{C}$ may deviate significantly from the annual mean. To account for this, Mulder & Syvitski (1995) used a sediment rating curve $Q_s = aQ^b$, where a and b are empirical coefficients that depend on the river and the averaging time. The exponent b in the rating curve is generally >1, but rarely exceeds 2.

Using rating curves, a drainage area–maximum flood relation (Matthai, 1990) and a critical sediment concentration C_c of ≈ 40 kg m^{-3} (required to render the density of the riverine outflow equal to that of sea water at the river mouth), Mulder & Syvitski (1995) classified rivers according to their capacity to generate a hyperpycnal plume. First, rivers with $C_c \leq 5\bar{C}$ were said to be 'dirty', as they could reasonably produce a hyperpycnal plume every year as a result of seasonal variations (assumed to a be a factor of 5) in sediment discharge. Only nine out of the 147 rivers could be called 'dirty', and most were small rivers in mountainous terrain. The other rivers were categorized by calculating a maximum flood discharge Q_{flood} from the drainage area and the relationship of Matthai (1990). Taking the ratio of the flood and mean annual sediment rating curves yields the expression $C_{flood} = \bar{C}(Q_{flood}/Q)^b$. The exponent b was varied until $C_{flood} > C_c$. Depending on the value of b required to produce $C_{flood} > C_c$, the return period of hyperpycnal plume formation was inferred. Small, easy-to-attain values of b were related to short return periods, whereas large b-values were indicative of relatively rare events. Although quantification by these means is questionable (Matthai, 1990), it provides a simple, rational way to classify rivers with limited data. The classifications were defined as follows: $b \leq 1$, moderately dirty (return periods of less than 100 years); $1 < b \leq 1{\cdot}5$, moderately clean (return periods of the order of hundreds of years); $1{\cdot}5 < b \leq 2$, clean (a return period of the order of tectonic/climatic timescales); $b > 2$, unlikely ever to produce a hyperpycnal plume.

The experiments reported here have demonstrated turbidity current/hyperpycnal plume generation to be possible with sediment concentrations 40 times less than those required to render the outflow heavy relative to the oceanic ambient (i.e. 1 kg m^{-3}). The critical concentration varied depending on the particular structure of the salinity and temperature field; consequently, a conservative estimate of the critical concentration, 5 kg m^{-3}, was used. At 5 kg m^{-3}, finger convection is at least as vigorous as observed floc settling (Fig. 4) and can generate convection for any realistic, stabilizing temperature stratification. Lowering the critical threshold C_c from 40 to

5 kg m^{-3} and using the same logic as Mulder & Syvitski (1995) suggests that 61 rivers produce hyperpycnal flows annually (Table 3). Most of the rivers previously characterized as 'moderately dirty' are now characterized as 'dirty'; among these are the Eel River and the larger rivers of New Zealand and Taiwan. The 61 rivers now characterized as dirty produce 53% of the world's oceanic sediment load and are therefore responsible for a significant portion of the sediment record.

CONCLUSIONS

Laboratory experiments indicate that hyperpycnal plumes can be formed with sediment concentrations as low as 1 kg m^{-3} under realistic oceanic river plume conditions (Fig. 3). Even when a more conservative critical concentration (5 kg m^{-3}) is used, many of the world's rivers appear capable of producing hyperpycnal plumes on an annual or decadal basis. Although direct observation of hyperpycnal plume formation from sediment-driven convection in a natural river plume has yet to be obtained, this physical phenomenon would provide a plausible explanation for the ubiquity of turbidite deposits in many deep-water environments.

ACKNOWLEDGEMENTS

Financial support for J.D.P. was provided by Chevron and for J.D.P. and J.P.S. by ONR-STRATAFORM. Dr Joseph Kravitz is thanked for the STRATAFORM support. Laboratory experiments were performed with the assistance of Andy Peabody, Juan Fedele and Jon Lubetsky. The authors thank Stuart Dalziel for generously donating the Rayleigh–Taylor tank. Special thanks to Marcelo García, Thierry Mulder, Arne Pearlstein and Gary Parker for their inspiring ideas on the subject. Brian Dade, David Hoyal and Jim Best provided valuable reviews that significantly improved the final manuscript.

NOTATION

a = linear coefficient in sediment rating curve
b = exponent in sediment rating curve
C = volumetric concentration of sediment
C_c = critical sediment concentration required to produce hyperpycnal plumes (M L^{-3})
C_{flood} = flood sediment concentration (M L^{-3})
C_{mass} = mass concentration of sediment (M L^{-3})
D_{50} = mean grain size of sediment (L)
Fr_c = density current Froude number, $U_c/\sqrt{\delta g h_c}$
g = gravitational acceleration (L T^{-2})
h_c = height (depth) of gravity current (L)
Q = mean annual river discharge (L^3 T^{-1})
Q_{flood} = volumetric river discharge during flood (L^3 T^{-1})
R = density-difference ratio $(\alpha \Delta T + \beta \Delta S)/\beta' C$
Ri = Richardson number, $\delta g h/\Delta U^2$
R_s = density-difference ratio neglecting the effect of temperature, $\beta \Delta S/\beta' C$
Re_c = density current Reynolds number, $U_c h_c/\nu$
Re_p = particle Reynolds number, $v_s D_{50}/\nu$
S = salinity
T = temperature
U = speed of vertically convecting fingers (L T^{-1})
U_c = front speed of gravity current (L T^{-1})
v_s = Stokes settling speed (L T^{-1})
α = conversion of temperature difference to density difference (T^{-1})
β = conversion of salinity difference to density difference
β' = conversion of volumetric sediment concentration to density difference
δ = density difference, $\alpha \Delta T + \beta \Delta S - \beta' C$
ΔT = temperature difference between upper and lower layer
ΔS = salinity difference between upper and lower layer
ν = kinematic viscosity (L^2 T^{-1})

REFERENCES

Beattie, P.D. and **Dade, W.B.** (1996) Is scaling in turbidite deposition consistent with forcing by earthquakes? *J. Sed. Res.*, **66**, 909–915.

Bradley, W.H. (1965) Vertical density currents. *Science*, **150**, 1423–1428.

Britter, R.E. and **Simpson, J.E.** (1978) Experiments on the dynamics of a gravity current head. *J. Fluid Mech.*, **88**, 223–240.

Chen, C.F. (1997) Particle flux through sediment fingers. *Deep-Sea Res.*, **44**, 1645–1654.

Dalziel, S.B. (1993) Rayleigh–Taylor instability – Experiments with image-analysis. *Dyn. Atmos. Oceans*, **20**, 127–153.

García, M.H. and **Parker, G.** (1993) Experiments on the entrainment of sediment into suspension by a dense bottom current. *J. Geophys. Res.*, **98**(C3), 4793–4807.

Geyer, W.R. and **Smith, J.D.** (1987) Shear instability in a highly stratified estuary. *J. Phys. Oceanogr.*, **17**, 1668–1679.

Green, T. (1987) The importance of double diffusion to the settling of suspended material. *Sedimentology*, **34**, 319–331.

Hill, P.S. and **Nowell, A.R.M.** (1995) Comparison of two models of aggregation in continental-shelf bottom boundary layers. *J. Geophys. Res.*, **100**, 22749–22763.

Hill, P.S., Syvitski, J.P.M., Cowan, E.A. and **Powell, R.D.** (1998) *In situ* observations of floc settling velocities in Glacier Bay, Alaska. *Mar. Geol.*, **145**, 85–94.

Howard, L.N. (1961) Note on a paper from John W. Miles. *J. Fluid Mech.*, **10**, 509–512.

Hoyal, D.C.J.D., Bursik, M.I. and **Atkinson, J.F.** (1999a) The influence of diffusive convection on sedimentation from buoyant plumes. *Mar. Geol.*, **159**, 205–220.

Hoyal, D.C.J.D., Bursik, M.I. and **Atkinson, J.F.** (1999b) Settling-driven convection: a mechanism of sedimentation from stratified fluids. *J. Geophys. Res.*, **104**, 7953–7966.

Huppert, H.E. and **Simpson, J.E.** (1980) Slumping of gravity currents. *J. Fluid Mech.*, **99**, 785–799.

Imran, J., Parker, G. and **Pirmez, C.** (1999) A nonlinear model of flow in meandering submarine and subaerial channels. *J. Fluid Mech.*, **400**, 295–331.

Keunen, Ph.H. (1968) Settling convection and grain-size analysis. *J. Sed. Petrol.*, **38**, 817–831.

Kineke, G.C., Sternberg, R.W., Trowbridge, J.H. and **Geyer, W.R.** (1996) Fluid-mud processes on the Amazon continental shelf. *Cont. Shelf Res.*, **16**, 667–696.

Kineke, G., Woolfe, K.J., Kuehl, S.A., Milliman, J., Dellapenna, T.M. and **Purdon, R.G.** (2000) Sediment export from the Sepik River, Papua New Guinea: Evidence for a divergent dispersal system. *Cont. Shelf Res.*, **20**, 2239–2266.

Kneller, B. (1995) Beyond the turbidite paradigm: Physical models for deposition of turbidites and their implications for reservoir prediction. In: *Characterization of Deep Marine Clastic Systems* (Eds A.J. Hartley and D.J. Prosser), *Geol. Soc. Lond. Spec. Publ.*, **94**, 31–49.

Maar, J.D.G. (1999) *Experiments on subaqueous sandy gravity flows: flow dynamics and deposit structures*. MSc Thesis, University of Minnesota.

Matthai, H.F. (1990) Floods. In: *The Geology of North America* (Eds M.G. Wolman and H.C. Riggs), **O-1**, pp. 97–120. Geological Society of America, Boulder, CO, USA.

Maxworthy, T. (1983) The dynamics of double-diffusive gravity currents. *J. Fluid Mech.*, **128**, 259–282.

Maxworthy, T. (1999) The dynamics of sedimenting surface gravity currents. *J. Fluid Mech.*, **392**, 27–44.

Morehead, M.D. and **Syvitski, J.P.** (1999) River plume sedimentation modeling for sequence stratigraphy: application of the Eel Shelf, California. *Mar. Geol.*, **154**, 29–41.

Mulder, T. and **Syvitski, J.P.M.** (1995) Turbidity currents generated at river mouths during exceptional discharges to the world oceans. *J. Geol.*, **103**, 285–299.

Normark, W.R., Posamentier, H. and **Mutti, E.** (1993) Turbidite systems: state of the art and future directions. *Rev. Geophys.*, **31**, 91–116.

Ogston, A.S., Cacchione, D.A., Sternberg, R.W. and **Kineke, G.C.** (2000) Observations of storm and river flood-driven sediment transport on the northern California continental shelf. *Cont. Shelf Res.*, **20**, 2141–2162.

Parker, G., Fukushima, Y. and **Pantin, H.M.** (1986) Self-accelerating turbidity currents. *J. Fluid Mech.*, **171**, 145–181.

Parsons, J.D. (1998) Mixing mechanisms in density intrusions. PhD Thesis, University of Illinois at Urbana-Champaign.

Parsons, J.D. and **García, M.H.** (2000) Enhanced sediment scavenging due to double-diffusive convection. *J. Sed. Res.*, **70**, 47–52.

Schmitt, R.W. (1994) Double diffusion in oceanography. *Annu. Rev. Fluid Mech.*, **26**, 255–285.

Sternberg, R.W., Berhane, I. and **Ogston, A.S.** (1999) Measurement of size and settling velocity of suspended aggregates on the Northern California continental shelf. *Mar. Geol.*, **154**, 43–53.

Syvitski, J.P.M. and **Hein, F.J.** (1991) Sedimentology of an arctic basin: Itirbilung Fjord, Baffin Island, Canada. *Geol. Assoc. Can. Prof. Pap.*, **91-11**, 67 pp.

Syvitski, J.P.M. and **Murray, J.W.** (1981) Particle interaction in fjord suspended sediment. *Mar. Geol.*, **39**, 215–242.

Thorpe, S.A. (1973) Experiments on instability and turbulence in a stratified shear flow. *J. Fluid Mech.*, **61**, 731–751.

Whitehouse, V.G., Jeffrey, L.M. and **Debrecht, J.O.** (1960) Differential settling tendencies of clay minerals in saline waters. *Clay Mineral.*, **8**, 1–79.

Zeng, J., Lowe, D.R., Prior, D.B., Wiseman, J., Jr and **Bornhold, B.D.** (1991) Flow properties of turbidity currents in Bute Inlet, British Columbia. *Sedimentology*, **38**, 975–996.

Manuscript received 29 March 2000;
revision accepted 21 November 2000.